PROCEEDINGS OF SCIENCE

Probing the strength of the intergalactic magnetic field through high-energy gamma-ray observations and modelling of hard and non-variable blazar sources

B. Bisschoff*[a], B van Soelen[a], P.J. Meintjes[a] and K.K. Singh[ab]

[a]*Department of Physics, University of Free State, PO Box 339, Bloemfontein, South Africa, 9300*
[b]*Astrophysical Sciences Division, Bhabha Atomic Research Centre, Mumbai 400085, India*
E-mail: bisschoffb@ufs.ac.za

Galaxies and galaxy clusters are separated by large distances of nearly empty regions of space called the intergalactic space. In these regions, a weak magnetic field is thought to be present and is predicted to be of a primordial (early universe) origin. The field is called the intergalactic magnetic field (IGMF) and knowledge about its strength, coherence length, and origin is limited. Understanding the origin of the IGMF is crucial because of the impact it may have had on an early star and galaxy formations. It has been proposed that the IGMF can be indirectly constrained through gamma-ray observations and SED analysis in the GeV-TeV energy range. TeV photons will undergo $\gamma\gamma$ absorption with the extra-galactic background light (EBL) and could initiate a cascade process, producing more emission at lower energies. However, the IGMF could deflect the electrons from the initial path and, therefore, the GeV-TeV energy emission may indirectly measure the magnetic field strength. In this paper, seven hard and non-variable BL Lacs were selected and reanalysed with the improved *Fermi*-LAT Pass 8 analysis pipeline. Using previous Imaging Atmospheric Cherenkov Telescopes (IACTs) observational results, the secondary cascade component was modelled using the ELMAG code of Kachelrieß (2012) and the Kneiske (2010) EBL model. From this, the total spectrum was determined by the sum of the cascade and primary (intrinsic) spectra, and consequently was compared to the *Fermi*-LAT spectrum, allowing constraints to be placed on the strength of the IGMF. We assumed that there is indeed a contributing cascade spectrum superimposed on the primary (intrinsic) spectrum and consequently used three different scenarios to constrain the IGMF strength namely: cascade dominant, primary dominant and a in-between scenario. All three scenarios were modelled with the cascade spectrum. In addition, the primary dominant scenario was also modelled with a power law (PL) model and the in-between scenario was modelled with a broken power law (BPL) model. These three scenarios allowed us to preliminary determine two lower limits (cascade and primary dominant spectra scenarios) and a best-fit (in-between scenario) value for the IGMF strength. Consequently, the IGMF strength was preliminary constrained with a lower limit between $4\times10^{-17}\lesssim B_{\rm LL}\,({\rm G})\lesssim 1\times10^{-15}$ and a best-fit value of $B_{\rm IGMF}\sim(6\pm1)\times10^{-17}$ G.

7th Annual Conference on High Energy Astrophysics in Southern Africa - HEASA2019
28 - 30 August 2019
Swakopmund, Namibia

*Speaker.

PoS(HEASA2019)048

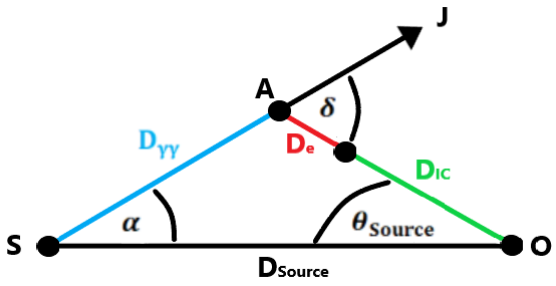

Figure 1. Illustration of electromagnetic cascading process that starts at A and ends at $A + D_e$, where D_e represents the electron cooling distance. The blazar jet, that originates at point S, is pointing in the direction of $S \rightarrow J$ that is misaligned with the line of sight of the observer O. $D_{\gamma\gamma}$ represents the $\gamma\gamma$ absorption mean free path and $D_{\rm IC}$ represents the final distance that the Inverse-Compton scattered photons will travel before reaching the observer at O.

1. Introduction

Magnetic fields have been observed to be universal for planets, stars, galaxies and galaxy clusters. Recent observational results indicate that even the intergalactic medium (IGM) could have a magnetic field, termed the intergalactic magnetic field (IGMF), with a field strength constrained between $10^{-19} < B_{\rm IGMF}\ ({\rm G}) < 10^{-9}$ and a coherence length ($\lambda_{\rm IGMF}$) up to Mpc scales [3, 4, 6].[1] The IGMF is predicted to be of primordial origin, with its field strength ($B'_{\rm IGMF}$) predicted to evolve with redshift as [7, 8]:

$$B'_{\rm IGMF}(z) = B_0(1+z)^2 \tag{1.1}$$

where B_0 is the present-day IGMF strength.

Gamma-ray observations of very-high-energy (VHE) emitting blazars provide one method to indirectly probe the IGMF, as is illustrated in Figure 1. Suppose that a blazar is situated at point S, with a relativistic jet which produces VHE gamma rays, initially travel along the path $S \rightarrow J$, and which is misaligned with the observer at point O. At point A, the gamma rays interact with the extra-galactic background light (EBL) photons to produce electron-positron pairs, which will preferentially travel in the same direction as the original gamma rays. These electron-positron pairs can then be deflected by the IGMF away from their original trajectory along the path $A \rightarrow O$, towards the observer. The angle by which the electron-positron pairs are deflected is δ and is highly dependent on the gamma-ray photon energy, the magnetic field strength and the coherence length of the IGMF. After the electron-positron pairs have traversed over a average distance of D_e, the electron-positron pairs will inverse Compton scatter cosmic microwave background (CMB) photons up to MeV/GeV energies. This secondary gamma-ray spectrum, originating from the up scattered CMB photons, will then be superimposed on the primary (intrinsic) gamma-ray spectrum of the source [8]. The deflection of the electron-positron pairs will result in an attenuation of the cascade emission which is dependent on the deflection angle (δ), EBL energy density (u_{EBL}) and the energy of the original VHE gamma rays.

[1] The coherence length ($\lambda_{\rm IGMF}$) describes the spatial structure of the IGMF and is defined as the average distance over which the magnetic field changes its orientation by 90 degrees.

2. HE and VHE Spectral Analysis

Ten years of *Fermi*-LAT Pass 8 data[2] (2008-09-01 - 2018-09-01) in the $0.1-300$ GeV energy range for seven hard and non-variable blazar sources were reanalysed, to test for variability and obtain spectral model parameters. The Fermi Science Tools package (version 1.0.5) was used to perform the spectrum model fitting with GTLIKE. For the background subtraction, the galactic diffuse (gll_iem_v06.fits) and extra-galactic isotropic (iso_P8R3_SOURCE_V2.txt) emission template files were also included in the source model file. None of the sources showed large variability in flux or the spectral shape.

It is necessary to determine the primary and total observed spectra, since we assume that the total observed *Fermi*-LAT spectrum consists of a superposition between the cascade and primary spectra. Therefore, the SED of each source was modelled in two different energy ranges, namely the cascade and primary dominant energy ranges. Neronov [9] found that if the cascade component is non-negligible, the cascade flux will be significant in the $\approx 0.1-10$ GeV energy range, and contrarily insignificant above ~ 10 GeV. Therefore, the cascade dominant energy range is adopted as $\approx 0.1-10$ GeV. In the second energy range the primary spectrum is the dominant contributor to the total observed spectrum, since the EBL attenuation is minimal.[3] In order to determine the second energy range, the energy at which the photon survival probability reaches $\approx 90\%$ was determined with the EBL absorption code created by M. Meyer with the Kneiske [2] EBL model.[4] Consequently, it was determined for all sources that the EBL attenuation becomes significant between $\approx 100-200$ GeV, which we adopt as the second energy range (primary dominant).

In these two energy ranges ($\approx 0.1-10$ GeV and $\approx 10-200$ GeV) the spectral analysis was performed, with the *Fermi*-LAT analysis, to obtain the power law (PL) spectrum model for each energy range. However, the two energy ranges were allowed to change depending on whether the likelihood fit, from the *Fermi*-LAT analysis, showed convergence or not. For 1ES 1218+304 and RBG J0152+017 the likelihood fit did not converge, and instead a PL model was fitted to the data with a chi-square fit to obtain the primary spectrum of the source.

The VHE ($E \gtrsim 100$ GeV) data for each source were de-absorbed with the Kneiske [2] EBL model.[5] A chi-squared fit was performed to the VHE de-absorbed data points to obtain a VHE PL spectrum. Then a chi-squared fit, for a broken power-law (BPL) model, was performed for the primary spectrum in the energy range $E > 10$ GeV. The PL photon indexes ($\Gamma_{10-200\ \mathrm{GeV}}$ and $\Gamma_{E>200\ \mathrm{GeV}}$), obtained for the primary source spectrum *Fermi*-LAT analysis (in the energy range $\approx 10-200$ GeV) and the VHE de-absorbed data chi-square fit, were used for the BPL indexes (Γ_1 and Γ_2), while the break energy (E_b) and normalisation (N_0) parameters for the BPL model were fitted. Table 1 shows all seven blazar sources with their names, redshifts and all the obtained spectral indexes. As an example, the obtained BPL and *Fermi*-LAT PL spectra, with the full energy range chi-square fit spectrum, are shown in Figure 2a for the source 1ES 0347-121.[6]

[2] *Fermi*-LAT data is available from: https://fermi.gsfc.nasa.gov/cgi-bin/ssc/LAT/LATDataQuery.cgi

[3] Note, the $\gamma\gamma$ absorption as a function of energy depends on the redshift and the considered EBL model.

[4] The EBL absorption code can be found at: https://github.com/me-manu/eblstud

[5] Note, the VHE data might not be contemporaneous with the *Fermi*-LAT data, and will be investigated in the future.

[6] The VHE data of the source 1ES 0347-121 can be found at [10].

Source	Redshift	PL index (Γ)		BPL indexes	
		$0.1-10$ GeV	$0.1-300$ GeV	Γ_1	Γ_2
1ES 0414+009	0.287	1.89 ± 0.01	1.86 ± 0.03	1.73 ± 0.27	1.86 ± 0.31
1ES 0347-121	0.188	1.76 ± 0.03	1.62 ± 0.04	1.27 ± 0.38	1.87 ± 0.15
1ES 1101-232	0.186	1.73 ± 0.02	1.67 ± 0.04	1.21 ± 0.26	1.76 ± 0.16
1ES 1218+304	0.182	1.71 ± 0.02	1.51 ± 0.04	1.60 ± 0.04	1.79 ± 0.03
1ES 0229+200	0.140	1.78 ± 0.32	1.60 ± 0.03	1.15 ± 0.74	1.65 ± 0.12
RGB J0710+591	0.125	1.68 ± 0.02	1.73 ± 0.04	1.37 ± 0.39	1.90 ± 0.18
RGB J0152+017	0.080	1.96 ± 0.16	1.96 ± 0.16	1.81 ± 0.03	1.81 ± 0.03

Table 1. Source names, redshifts and the obtained photon indexes for the seven hard and non-variable blazar sources.

3. Modelling the Cascade Emission

The secondary cascade component was modelled with the ELMAG code of Kachelrieß [1][7], by using the EBL model of Kneiske [2, 11]. For simplicity, the secondary cascade spectrum was modelled by assuming a coherence length of 1 Mpc and that all the BL Lac sources have been emitting relatively constant flux over $\gtrsim 10^6$ years, as was done by [4, 12, 13].[8] The VHE part of the primary spectrum ($\gtrsim 100$ GeV) was used as the input spectrum to model the secondary cascade spectrum.[9] Photons deflected outside the *Fermi*-LAT point spread function are removed from the simulation [4, 14]. The total spectrum flux is obtained by adding the primary and cascade spectra, as shown in Figure 2b for the SED of the source 1ES 0347-121.

4. Results and Discussion

We place preliminary constraints on the IGMF strength by considering three different scenarios: cascade spectrum dominating scenario (lower limit), primary spectrum dominating scenario (lower limit) and a in-between (best-fit) scenario.

A lower limit on the IGMF strength can be obtained in the case when the cascade spectrum is the dominating contributor to the total observed spectrum (cascade dominating scenario). This can be done by not allowing the cascade spectrum to exceed the *Fermi*-LAT flux by more than one standard deviation. The minimum IGMF strength value that satisfies the latter condition was then used as the lower limit for each source. Then the minimum lower limit value ($B_{\rm IGMF} > 6\times10^{-17}$ G for a redshift of $z = 0.188$), between the sources was used with equation 1.1 to determine the IGMF strength lower limit of $B_{\rm IGMF} \gtrsim 4\times10^{-17}$ G. This agrees with the lower limits of $B_{\rm IGMF} \gtrsim 10^{-19}$ G and $B_{\rm IGMF} \gtrsim 3\times10^{-17}$ G, that Finke et al. [4] and Tanaka et al. [5] previously found.

An alternative method to place a limit on the IGMF strength can be obtained in the case when the primary spectrum is the dominating contributor to the total observed spectrum (primary domi-

[7]The ELMAG code and its user manual can be found at: http://elmag.sourceforge.net.

[8]By assuming that the blazar is only stable on shorter time scales (~ 2 years), the IGMF strength lower limit decreases ($B_{\rm IGMF} \sim 10^{-18}$ G) [15].

[9]The ELMAG code uses a Monte Carlo method to model the full cascade process and spectrum.

Source	IGMF strength (G)		
	Best-fit	Cascade Dominating	Primary Dominating
1ES 0414+009	$\text{NA} \leq \text{B} \leq 5 \times 10^{-16}$	NA	2×10^{-15}
1ES 0347-121	$9 \times 10^{-17} \leq B \leq 3 \times 10^{-16}$	6×10^{-17}	3×10^{-14}
1ES 1101-232	$9 \times 10^{-17} \leq B \leq 2 \times 10^{-16}$	6×10^{-17}	5×10^{-15}
1ES 1218+304	$6 \times 10^{-17} \leq B \leq 9 \times 10^{-17}$	NA	7×10^{-15}
1ES 0229+200	NA	NA	3×10^{-14}
RGB J0710+591	$8 \times 10^{-17} \leq B \leq 2 \times 10^{-16}$	3×10^{-17}	2×10^{-15}
RGB J0152+017	$\text{NA} \leq \text{B} \leq 1 \times 10^{-16}$	NA	3×10^{-15}

Table 2. Preliminary obtained IGMF strength values for the three different fits: best-fit, cascade and primary dominant (lower limits). NA shows that no good fit could be obtained for any magnetic field strength within one standard deviation of the *Fermi*-LAT PL model.

nating scenario). This can be done by fitting a PL spectrum through the HE and VHE data points, which is then used as the primary spectrum. The cascade spectrum was used to find another limit on the IGMF strength by not allowing the sum of the cascade spectrum and the newly obtained primary spectrum to exceed the *Fermi*-LAT flux by more than one standard deviation. The minimum IGMF strength value was then used to constrain the IGMF strength for every source. The minimum value ($B_{\text{IGMF}} > 2 \times 10^{-15}$ G for a redshift of $z = 0.287$), between the sources, was used with equation 1.1 to limit the IGMF strength to $B_{\text{IGMF}} \gtrsim 10^{-15}$ G. This agrees with the lower limit $B_{\text{IGMF}} \gtrsim 10^{-15}$ G [15, 16].

For the best-fit scenario, it is assumed that a cascade component is superimposed on the primary spectrum of the source. For each source the BPL model, with spectral indexes $\Gamma_{10-200\text{ GeV}}$ and $\Gamma_{E>200\text{ GeV}}$, is used as the primary source spectrum and added to the cascade spectrum to obtain the total spectrum. The IGMF strength values were obtained by fitting the *Fermi*-LAT PL model in the $\approx 0.1 - 10$ GeV energy range with the total spectrum. All the obtained IGMF strength values are shown in Table 2 for all three scenarios.

5. Conclusion

All the obtained IGMF strength values in Table 2 were plotted in Figure 2c. The best-fit data points were then modelled with the IGMF strength evolution equation (Equation 1.1). If the obtained BPL primary (intrinsic) spectrum from the *Fermi*-LAT analysis truly represents the source primary (intrinsic) spectrum, and there is a non-negligible cascade spectrum superimposed on the primary (intrinsic) spectrum, then the present day IGMF strength was preliminary determined as $B_{\text{IGMF}} \sim (6 \pm 1) \times 10^{-17}$ G with the best-fit scenario. Otherwise, only limits can be obtained from the most dominant spectrum (primary or cascade spectrum) contributor scenario. The preliminarily determined lower limits of $4 \times 10^{-17} \lesssim B_{\text{LL}}\ (\text{G}) \lesssim 1 \times 10^{-15}$ are within the range of values previously found.

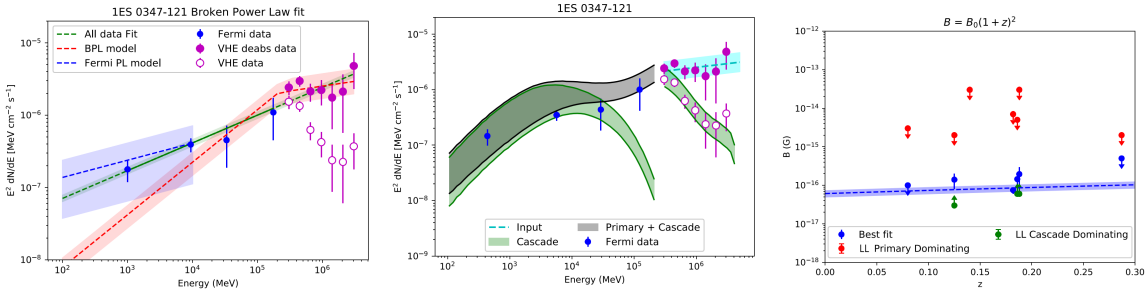

(a) The obtained BPL primary (red), *Fermi*-LAT PL model (blue) and full fit (green) spectra with the HE (blue) and VHE (magenta) data points.

(b) The input (cyan) and output cascade (green) spectra. The total (black) spectrum is compared to the observed *Fermi*-LAT (blue) data points.

(c) IGMF evolution model (blue) shown with the data points for the cascade (green), primary (red) dominating and best-fit (blue) scenarios.

Figure 2. The modelled SED plots, for the source 1ES 0347-121, and IGMF strength plots.

6. Acknowledgements

The financial assistance of the National Research Foundation (NRF) towards this research is hereby acknowledged. The *Fermi*-LAT analysis was performed using the University of the Free State High-Performance Computing Unit.

References

[1] M. Kachelrieß et al., *Computer Physics Communications* **183** (2012) 4

[2] T.M. Kneiske et al., *A&A* **515** (2010) A19

[3] F. Govoni et al., *Science* **364** (2019) 4

[4] J.D. Finke et al., *ApJ* **814** (2015) 1

[5] Y.T. Tanaka et al., *ApJ* **787** (2014) 2

[6] M.S. Pshirkov et al., *PhRvL* **116** (2016) 19

[7] D. Grasso et al., *PhR.* **348** (2001) 163

[8] A. Neronov et al., *Phys. Rev. D* **80** (2009) 123012

[9] A. Neronov et al., *ApJ* **757** (2011) 61

[10] F. Aharonian et al., *A&A* **473** (2007) 3

[11] K.K. Singh et al., *NewA* **27** (2014) 34

[12] K. Dolag et al., *ApJ* **727** (2011) L4

[13] C.D. Dermer, *ApJ* **733** (2011) 2

[14] M. Ackermann et al., *ApJS* **237** (2018) 2

[15] A.M. Taylor et al., *A&A* **529** (2011) A144

[16] F. Tavecchio et al., *MNRAS* **414** (2011) 4